

Collective flows of α -clustering $^{12}\text{C} + ^{197}\text{Au}$ by using different flow analysis methods

S. Zhang,¹ Y. G. Ma*,^{1,2,3} J. H. Chen,¹ W. B. He,⁴ and C. Zhong¹

¹*Shanghai Institute of Applied Physics, Chinese Academy of Sciences, Shanghai 201800, China*

²*University of Chinese Academy of Sciences, Beijing 100049, China*

³*ShanghaiTech University, Shanghai 200031, China*

⁴*Institute of Modern Physics, Fudan University, Shanghai 200433, China*

(Dated: September 26, 2021)

Recently the ratio of triangular flow to the elliptic flow (v_3/v_2) of hadrons was proposed as a probe to detect the pattern of α -clustering ^{12}C in $^{12}\text{C}+^{197}\text{Au}$ collisions at relativistic energy by a participant plane method (Phys. Rev. C 95, 064904 (2017)). In experimental event plane method, Q-cumulant method and two-particle correlation method with rapidity gap always were used for measurement of collective flow only by means of momentum space. By comparing collective flow through the different methods, the ratio of v_3/v_2 could be taken as an experimental probe to distinguish different α -clustering structure of ^{12}C .

PACS numbers: 25.75.Gz, 12.38.Mh, 24.85.+p

I. INTRODUCTION

In relativistic heavy-ion collisions, initial geometry distribution can affect some observables, such as collective flows [1–4], Hanbury-Brown-Twiss (HBT) correlation [5, 6] and fluctuation [7]. The initial geometry distribution was always influenced by initial dynamical fluctuation and intrinsic structure in the collided nuclei. These effects have been extensively investigated by different models, such as hydrodynamical models [8–11] as well as in transport models [12–16], respectively. Initial fluctuation effects have been also proposed on some observables or physics quantities, such as on collective flows [17–19], conserved quantities [20], density fluctuations [21], and charge separation [22]. In References [12, 13] the carbon was considered with 3- α structure and collided against a heavy nucleus at very high energies and the results implied the final collective flow was sensitive to the initial geometry distribution.

In one of our recent papers [23] collective flow ratio of v_3/v_2 (here v_3 is the triangular flow and v_2 is elliptic flow) was proposed as a probe to detect the intrinsic structure of α -clustering nuclei with an α -clustered ^{12}C colliding against heavy-ion by using a multi-phase transport (AMPT) model. The α -cluster model which was originally proposed by Gamow [24] considered some light nuclei made of N- α , such as ^{12}C with 3- α and ^{16}O with 4- α . It was suggested that α clustering configurations can be identified by giant dipole resonance [25, 26] or photonuclear reaction in quasi-deuteron region [27, 28] by EQMD model calculations. Theoretically, ^{12}C could exhibit triangular or chain distribution of three α clusters and ^{16}O could present kite, chain or square arrangement of four α clusters in some specific conditions.

In our previous work [23] the participant plane (PP-

) method [29–31] was employed to calculate the collective flow. The PP-method always was used in theoretical analysis for initial geometry fluctuation effect on collective flow. Event plane (EP-) method [32–36], Q-cumulant (QC-) method [14, 15, 35, 37] and two particle correlation (2PC-) method with rapidity gap [38–42] were performed in this work to calculate collective flow of final charged hadrons as that in experiments. The results implied that centrality dependence of ratio of v_3/v_2 from 2PC-method was consistent with that from PP-method.

II. MODEL AND CALCULATION METHODS

The phase space of the collision system was simulated by a multi-phase transport model (AMPT) [43]. AMPT was developed to simulate heavy-ion collisions in a wide colliding energy range from SPS to LHC and successful to describe physics in relativistic heavy-ion collision for RHIC [43] and LHC [44], including pion-HBT correlations [45], di-hadron azimuthal correlations [46], collective flow [47, 48] and strangeness production [49, 50]. In this model, the initial state was simulated by HIJING model [51, 52], and the melted partons would interact with each other in a parton cascade model (ZPC) [53], and then hadrons formed by a simple quark coalescence model participate in hadronic rescattering through a relativistic transport (ART) model [54]. The initial nucleon distribution in ^{12}C was configured in HIJING model [51, 52] originally with pattern of Woods-Saxon distribution. And the other two cases of configuration of ^{12}C structure were performed as, three α clusters either in chain structure or in triangle structure. The parameters for the α -clustered ^{12}C were from calculation by EQMD model [25, 26, 55] and discussed in our previous work [23] in detail. Then we can obtain the phase space in $^{12}\text{C}+^{197}\text{Au}$ collisions at $\sqrt{s_{NN}} = 200$ GeV for flow calculation by using AMPT model.

The final particle azimuthal distribution can be ex-

*Author to whom all correspondence should be addressed: ygma@sinap.ac.cn

panded as [32, 33],

$$E \frac{d^3 N}{d^3 p} = \frac{1}{2\pi} \frac{d^2 N}{p_T dp_T dy} \times \left(1 + \sum_{i=1}^N 2v_n \cos[n(\phi - \Psi_{RP})] \right), \quad (1)$$

where E is the energy, p_T is transverse momentum, y is rapidity, ϕ is azimuthal angle of the particle. Ψ_{RP} is reaction plane angle. And the Fourier coefficients $v_n (n = 1, 2, 3, \dots)$ are collective flow to characterize different orders of azimuthal anisotropies with the form,

$$v_n = \langle \cos(n[\phi - \Psi_{RP}]) \rangle, \quad (2)$$

where the bracket $\langle \rangle$ denotes statistical averaging over particles and events. The true reaction plane angle Ψ_{RP} always is estimated by event plane angle [32–36] or by participant plane angle [29–31]. The harmonic flow can be calculated with respect to participant plane angle or event plane angle, called participant plane (PP-) method and event plane (EP-) method, respectively. Some method avoiding to reconstruct the reaction plane were developed, such as Q-cumulant (QC-) method [14, 15, 35, 37] and two particle correlation (2PC-) method with rapidity gap [38–42].

In participant coordinates system, the participant plane angle $\Psi_n\{PP\}$ can be defined by the following equation [29–31],

$$\Psi_n\{PP\} = \frac{\tan^{-1} \left(\frac{\langle r^2 \sin(n\phi_{part}) \rangle}{\langle r^2 \cos(n\phi_{part}) \rangle} \right) + \pi}{n}, \quad (3)$$

where, $\Psi_n\{PP\}$ is the n th-order participant plane angle, r and ϕ_{part} are coordinate position and azimuthal angle of participants in the collision zone at initial state, and the average $\langle \dots \rangle$ denotes density weighting. And then the harmonic flow coefficients with respect to participant plane angle are defined as,

$$v_n \equiv \langle \cos(n[\phi - \Psi_n\{PP\}]) \rangle. \quad (4)$$

PP-method has been used to calculate collective flow in some theoretical works [8–11, 14–16, 29–31]. And it always was applied to discuss the initial geometry fluctuation effect on collective flow since the participant plane angle $\Psi_n\{PP\}$ was constructed by initial energy distribution in coordinates space with the event-by-event fluctuation effects.

Event plane (EP-) method always was used in experimental analysis for harmonic flow coefficients and the event plane angle $\Psi_n\{EP\}$ was defined by [32–36]

$$\begin{aligned} Q_x &\equiv \sum_i^M \omega_i \cos(n\phi_i), \\ Q_y &\equiv \sum_i^M \omega_i \sin(n\phi_i), \\ \Psi_n\{EP\} &= \frac{1}{n} \tan^{-1} \left(\frac{Q_y}{Q_x} \right), \end{aligned} \quad (5)$$

where ϕ_i and ω_i are azimuthal angle and weight for the i th particle, respectively. In this work, the weight was chosen as unit. The sums extended over all particles used in the event plane reconstruction. Then harmonic flow coefficients could be calculated by

$$\begin{aligned} v_n &= \frac{v_n^{obs}}{\text{Res}\{\Psi_n\{EP\}\}}, \\ v_n^{obs} &= \langle \cos(km(\phi - \Psi_n\{EP\})) \rangle, \\ \text{Res}\{\Psi_n\{EP\}\} &= \langle \cos(km(\Psi_n\{EP\} - \Psi_{RP})) \rangle. \end{aligned} \quad (6)$$

The angular brackets indicate an average over all particles in all events and $km = n$ in this work. The resolution of event plane angle $\text{Res}\{\Psi_n\{EP\}\}$ owing to finite number of particles can be calculated by,

$$\begin{aligned} \text{Res}\{\Psi_n\{EP\}\} &= \langle \cos(km(\Psi_n\{EP\} - \Psi_{RP})) \rangle \\ &= \frac{\sqrt{\pi}}{2\sqrt{2}} \chi_m \exp(-\chi_m^4/4) I_{km} \\ I_{km} &= I_{(k-1)/2} \chi_m^2/4 + I_{(k+1)/2} \chi_m^2/4, \end{aligned} \quad (7)$$

χ_m could be estimated by sub-event method. The event used to calculate event plane angle would randomly be splitted into two sub-events, event A and B , with maximum difference of particle number equal to 1. χ_m from sub-event resolution $\langle \cos(km(\Psi_m^A - \Psi_m^B)) \rangle$ multiplying $\sqrt{2}$ would be the χ_m for full event resolution $\text{Res}\{\Psi_n\{EP\}\}$. The detail for this analysis can be found in references [33–36].

To avoid reconstructing the event plane and eliminating non-flow contribution, multi-particle correlation method was developed to calculate the harmonic flow, such as Q-cumulant (QC-) method [14, 15, 35, 37] and two particle correlation (2PC-) method with rapidity gap [38–42]. The multi-particle cumulant can be calculated directly from a Q vector,

$$Q_n = \sum_{i=1}^M e^{in\phi_i}, \quad (8)$$

where ϕ_i is azimuthal angle of particles in momentum space. The two- and four- particle cumulants can be written as

$$\begin{aligned} \langle 2 \rangle &= \langle e^{in(\phi_1 - \phi_2)} \rangle = \frac{|Q_n|^2 - M}{M(M-1)}, \\ \langle 4 \rangle &= \langle e^{in(\phi_1 + \phi_2 - \phi_3 - \phi_4)} \rangle \\ &= \{ |Q_n|^4 + |Q_{2n}|^2 - 2\text{Re}[Q_{2n}Q_n^*Q_n^*] \\ &\quad - 2[2(M-2)|Q_{2n}|^2 - M(M-3)] \} \\ &\quad / [M(M-1)(M-2)(M-3)]. \end{aligned} \quad (9)$$

Then, the average over all events can be formulated as

$$\begin{aligned} \langle \langle 2 \rangle \rangle &= \langle \langle e^{in(\phi_1 - \phi_2)} \rangle \rangle = \frac{\sum_{event} (W_{\langle 2 \rangle})_i \langle 2 \rangle_i}{\sum_{event} (W_{\langle 2 \rangle})_i}, \\ \langle \langle 4 \rangle \rangle &= \langle \langle e^{in(\phi_1 + \phi_2 - \phi_3 - \phi_4)} \rangle \rangle = \frac{\sum_{event} (W_{\langle 4 \rangle})_i \langle 4 \rangle_i}{\sum_{event} (W_{\langle 4 \rangle})_i}. \end{aligned} \quad (10)$$

And then the two- and four-particle cumulants, and the flow can be written as,

$$\begin{aligned} c_n\{2\} &= \langle\langle 2 \rangle\rangle, \\ c_n\{4\} &= \langle\langle 4 \rangle\rangle - 2 \times \langle\langle 2 \rangle\rangle^2, \\ v_n\{2\} &= \sqrt{c_n\{2\}}, \\ v_n\{4\} &= \sqrt[4]{-c_n\{4\}}. \end{aligned} \quad (11)$$

The above flow $v_n\{2\}$ and $v_n\{4\}$ is the reference flow with integration over transverse momentum p_T . The differential flow as a function of p_T will not be discussed here. The detail for the algorithm of Q-cumulant method can be found in references [14, 15, 35, 37].

In the 2PC-method [38–42], the two-dimensional (2D) two-particle correlation function is generally defined as

$$C(\Delta\phi, \Delta\eta) = \frac{S(\Delta\phi, \Delta\eta)}{B(\Delta\phi, \Delta\eta)}, \quad (12)$$

where

$$\begin{aligned} S(\Delta\phi, \Delta\eta) &= \frac{dN}{d\Delta\phi d\Delta\eta}, \\ B(\Delta\phi, \Delta\eta) &= \frac{dN}{d\Delta\phi d\Delta\eta}. \end{aligned} \quad (13)$$

$S(\Delta\phi, \Delta\eta)$ and $B(\Delta\phi, \Delta\eta)$ are the same-event pair distribution and the combinatorial distribution in two-particle phase space ($\Delta\phi = \phi_a - \phi_b$, $\Delta\eta = \eta_a - \eta_b$), respectively. Mix-event method is employed to calculate $B(\Delta\phi, \Delta\eta)$. In mix-event the pair particles are from two different events with similar event properties such as number of track. To reduce non-flow contribution at $(\Delta\phi, \Delta\eta) \sim (0, 0)$, a one-dimensional (1D) $\Delta\phi$ correlation function can be given with $2 < |\Delta\eta| < 5$. The 1D two-particle correlation function is generally defined as

$$C(\Delta\phi) = A \frac{\int S(\Delta\phi, \Delta\eta) d\Delta\eta}{\int B(\Delta\phi, \Delta\eta) d\Delta\eta}. \quad (14)$$

The normalization constant A is determined by scaling the number of pairs in $2 < |\Delta\eta| < 5$ to be the same between the same event counts (S) and the mix-event counts (B) [38]. And the distribution of pairs in $\Delta\phi$ can be expanded into a Fourier series,

$$\frac{dN_{pairs}}{d\Delta\phi} \propto 1 + 2 \sum_{n=1}^{\infty} v_{n,n} (p_T^a, p_T^b) \cos(n\Delta\phi). \quad (15)$$

The coefficients $v_{n,n}$ can be calculated directly by

$$v_{n,n} = \langle \cos(n\Delta\phi) \rangle = \frac{\sum_{m=1}^N \cos(n\Delta\phi_m) C(\Delta\phi_m)}{\sum_{m=1}^N C(\Delta\phi_m)}, \quad (16)$$

where $n = 2, 3$, and $N=200$ is the number of $\Delta\phi$ bins. The harmonic flow coefficients v_n ($n = 2, 3$) can be calculated as $v_n = v_{n,n} / \sqrt{|v_{n,n}|}$. The detail of this method can be found from references [38].

The above introduced method will be applied to calculate the harmonic flow in $^{12}\text{C}+^{197}\text{Au}$ collisions at $\sqrt{s_{NN}} = 200$ GeV for different configuration of ^{12}C structure.

III. RESULTS AND DISCUSSION

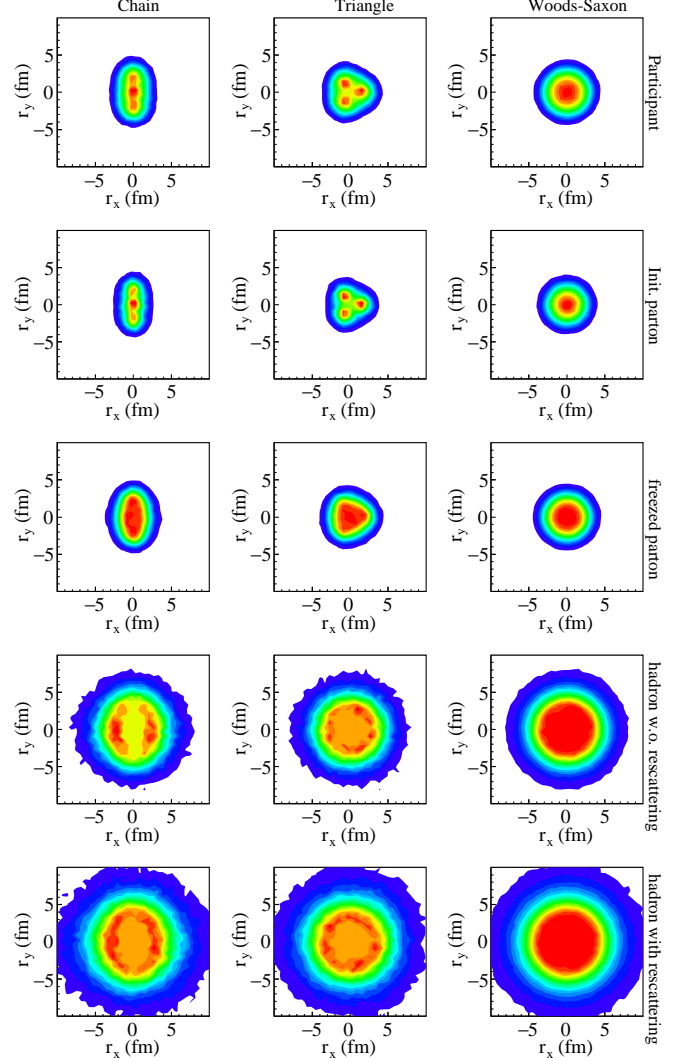


FIG. 1: (color online) In $^{12}\text{C}+^{197}\text{Au}$ collisions at $\sqrt{s_{NN}} = 200$ GeV, the distribution in X-Y plane of participants (first row), initial partons (second row), frozen partons (third row), hadrons without hadronic rescattering (fourth row) and hadrons with hadronic rescattering (fifth row) for different α -clustering configuration of ^{12}C structure, i.e., chain (left column), triangle (middle column), and Woods-Saxon (right column) structures.

Figure 1 shows the distribution in X-Y plane for participants, initial partons, frozen partons, hadrons without hadronic rescattering and hadron with hadronic rescattering in $^{12}\text{C}+^{197}\text{Au}$ collisions at $\sqrt{s_{NN}} = 200$ GeV for different configuration of ^{12}C structure. The initial nucleon distribution in ^{12}C is configured for (a) three α clusters in Chain structure, (b) three α clusters in Triangle structure, and (c) nucleons in Woods-Saxon distribution from HIJING model [51, 52] (Woods-Saxon). The distribution of radial centre of the α clusters in ^{12}C is

assumed to be a Gaussian function, $e^{-0.5\left(\frac{r-r_c}{\sigma_{r_c}}\right)^2}$, here r_c is average radial center of an α cluster and σ_{r_c} is the width of the distribution. And the nucleon inside each α cluster will be given by Woods-Saxon distribution. The parameters of r_c and σ_{r_c} can be obtained from the EQMD calculation [25–28]. For the Triangle structure, $r_c = 1.8$ fm and $\sigma_{r_c} = 0.1$ fm. For Chain structure, $r_c = 2.5$ fm, $\sigma_{r_c} = 0.1$ fm for two α clusters and the other one will be at the center in ^{12}C . Once the radial centre of the α cluster is determined, the centers of the three clusters will be placed in an equilateral triangle for the Triangle structure or in a line for Chain structure.

The participant plane angle $\Psi_n\{PP\}$ is reconstructed by using the coordinates from initial parton (the second row panels) instead of participants (the first row panels) for considering dynamical fluctuation from the initial collisions in HIJING model. These plots show X-Y coordinates distribution with respective to participant plane angle $\Psi_n\{PP\}$ and the events are selected for impact parameter $b = 0$ fm. After parton cascade (the third row panels), hadronization (the fourth row panels) and hadronic rescattering (the fifth row panels), the coordinates distributions in X-Y plane of production gradually tend to be thermalized. Similarly it was calculated for the distribution in p_x - p_y plane as shown in figure 2 with transverse momentum p_T window (0.2,3) GeV/c and rapidity window (-1,1). Note that there is no p_x - p_y distribution of participants since their momenta along beam direction (z-axis). For the chain structure, we can see that the p_x - p_y distribution is symmetrical for the initial partons and becomes asymmetrical after parton cascade (freezed parton) and this asymmetrical distribution is inherited by hadrons (without and with hadronic rescattering). For the triangle and Woods-Saxon distribution, there is no obvious evolution of azimuthal asymmetry at different stage which will be investigated by harmonic flow coefficients in the following. The flow formation mechanism was investigated in some works [56, 57]. The escape mechanism and contribution from parton collision time to collective flow were suggested in these work. From these viewpoints, p_x - p_y distribution will evolve from geometrical asymmetry to momentum asymmetry in transverse plane, which is obvious in the chain structure or in semi-central Au+Au collisions. And the following results will be calculated for final charged hadrons to investigate harmonic flow coefficients as did in experiments.

Figure 3 presents the second and third order event plane angle resolution $\text{Res}\{\Psi_n\{EP\}\}$ as a function of N_{track} in $^{12}\text{C}+^{197}\text{Au}$ collisions at $\sqrt{s_{NN}} = 200$ GeV for different configuration of ^{12}C structure. N_{track} is calculated in the rapidity window ($-2 < y < 2$) and transverse momentum window ($0.2 < p_T < 6$) GeV/c for the charged pion (π^\pm), Kaon (K^\pm) and proton (p, \bar{p}). The event plane angle resolution $\text{Res}\{\Psi_n\{EP\}\}$ increases with the increasing of N_{track} . The second (third) order event plane resolution is higher for chain (triangle) structure than for other patterns. These indicate that

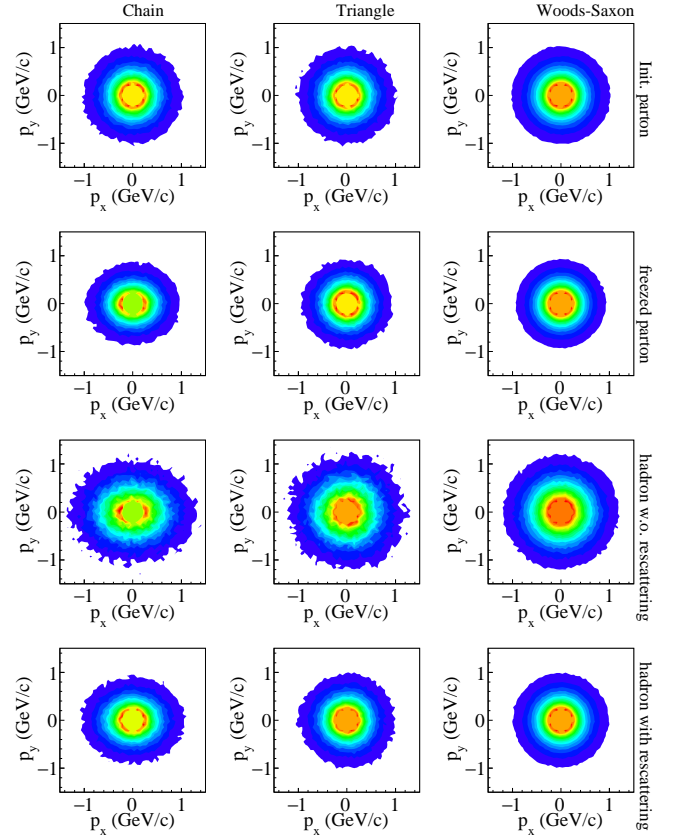


FIG. 2: (color online) In $^{12}\text{C}+^{197}\text{Au}$ collisions at $\sqrt{s_{NN}} = 200$ GeV, the distribution in p_x - p_y plane of initial partons (first row), freezed partons (second row), hadrons without hadronic rescattering (third row) and hadrons with hadronic rescattering (fourth row) for different α -clustering configuration of ^{12}C structure, i.e., chain (left column), triangle (middle column), and Woods-Saxon (right column) structures.

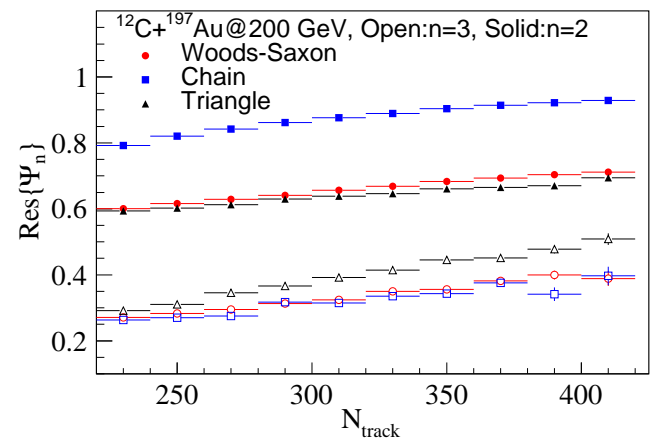


FIG. 3: (color online) In $^{12}\text{C}+^{197}\text{Au}$ collisions at $\sqrt{s_{NN}} = 200$ GeV, the second and third order event plane angle resolution as a function of N_{track} for different configuration of ^{12}C structure.

the event plane angle resolution depends not only on the number of particles used to reconstruct the event plane but also on the harmonic flow coefficients for the event plane angle which is determined by the harmonic flow coefficients itself [33–36].

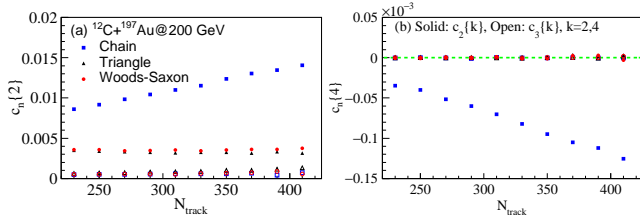


FIG. 4: (color online) In $^{12}\text{C}+^{197}\text{Au}$ collisions at $\sqrt{s_{NN}} = 200$ GeV, the two- and four-particle cumulants $c_n\{2\}$ and $c_n\{4\}$ as a function of N_{track} for different configuration of ^{12}C structure.

For the Q-cumulant (QC-) method, we investigated the two- and four-particle cumulants $c_n\{2\}$ and $c_n\{4\}$ as a function of N_{track} in $^{12}\text{C}+^{197}\text{Au}$ collisions at $\sqrt{s_{NN}} = 200$ GeV for different configurations of ^{12}C structure, as shown in figure 4. From panel (a) in figure 4 we can see that $c_2\{2\}$ increases rapidly for chain structure and $c_3\{2\}$ slightly increases with the increasing of N_{track} for triangle structure, respectively, and $c_n\{2\}$ ($n = 2, 3$) keeps almost flat for other cases. Unfortunately the four-particle cumulants $c_n\{4\}$ only give the reasonable value (< 0 for $v_n\{4\}$ in formula (11)) of $c_2\{4\}$ in chain structure pattern then only $v_n\{2\}$ is presented by QC-method. Obviously this method for calculation of multi-particle cumulants depends not only on the N_{track} but also on the asymmetrical flow itself [14, 15, 35, 37].

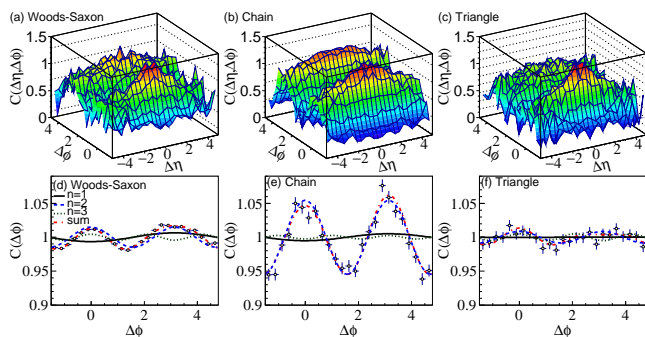


FIG. 5: (color online) In $^{12}\text{C}+^{197}\text{Au}$ collisions at $\sqrt{s_{NN}} = 200$ GeV, the two particle correlation function (rebinned into 25 bins) for different configuration of ^{12}C structure, $N_{\text{track}} > 200$ and $1 < p_T < 3$ GeV/c.

Figure 5 shows the 2D $\Delta\eta - \Delta\phi$ and 1D $\Delta\phi$ two particle correlation functions for different configurations of ^{12}C structure with $N_{\text{track}} > 200$ and $1 < p_T < 3$ GeV/c in $^{12}\text{C}+^{197}\text{Au}$ collisions at $\sqrt{s_{NN}} = 200$ GeV. The short range correlation at $(\Delta\phi, \Delta\eta) \sim (0, 0)$ suggests that there are autocorrelations from jet fragmentation and resonance decays [38–42] as shown at panels (a), (b) and (c)

in figure 5, so-called the non-flow contribution. We can see that the correlation function of Woods-Saxon (panel a) case is similar to that of Triangle (panel c) case. This similar distribution was found in $px - py$ distribution of final particles shown in figure 2 (bottom line). The panel (b) in figure 5 presents strong correlation near $\Delta\phi = 0$ and $\Delta\phi = \pi$, which is mainly from the flow contribution. The non-flow contribution was reflected near $(\Delta\phi, \Delta\eta) \sim (0, 0)$ since jet quenching and resonance decay always happen in a narrow $(\Delta\phi, \Delta\eta)$ space, namely short range correlation. To eliminate the non-flow contribution, 1D $\Delta\phi$ correlation functions presented at panels (d), (e) and (f) in figure 5 are obtained through integrating 2D $\Delta\eta - \Delta\phi$ correlation function with a large $\Delta\eta$ gap ($\Delta\eta > 2$). At panels (d), (e) and (f), the lines are contributions from the individual $v_{n,n}$ components ($n = 1, 2, 3$) and their sum as in formula (15) and the markers are from AMPT model. And then the harmonic flow can be calculated by using formula (16).

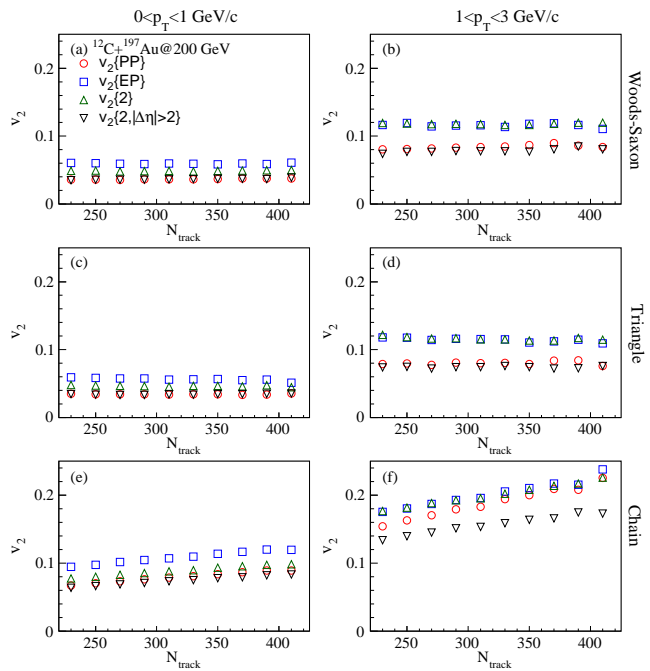


FIG. 6: (color online) In $^{12}\text{C}+^{197}\text{Au}$ collisions at $\sqrt{s_{NN}} = 200$ GeV, the elliptic flow v_2 by using different methods for different configuration of ^{12}C structure.

With the above introduced method for flow calculation, the elliptic and triangular flow are calculated and presented in figure 6 and figure 7 separately. $v_n\{PP\}$, $v_n\{EP\}$, $v_n\{2\}$ and $v_n\{2, |\Delta\eta| > 2\}$ denote the harmonic flow coefficients are calculated by PP-method, EP-method, QC-method and 2PC-method, respectively. Note that there is no $v_n\{4\}$ results by QC-method since the cumulant of $c_n\{4\}$ is unreasonable but in chain structure as shown in figure 4 (b). The trend of N_{track} dependence for the elliptic flow by using different method are consistent with each other. The elliptic flow (figure 6) in Woods-Saxon and triangle cases keep a flat N_{track} depen-

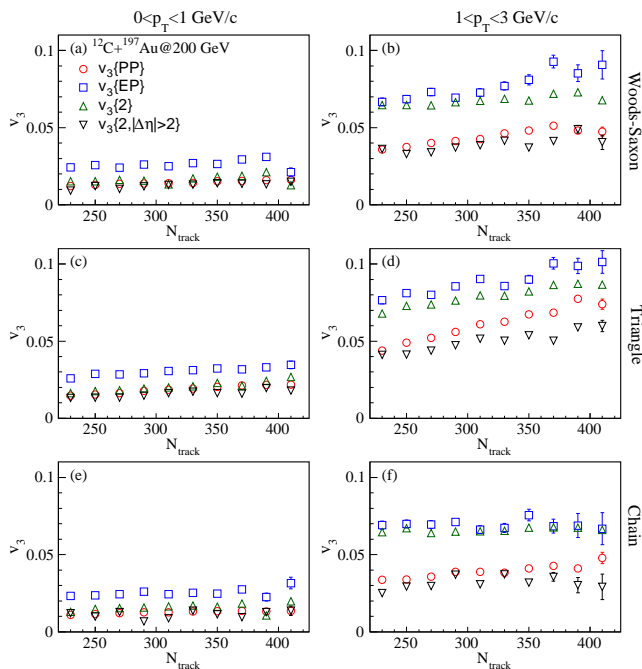


FIG. 7: (color online) In $^{12}\text{C}+^{197}\text{Au}$ collisions at $\sqrt{s_{NN}} = 200$ GeV, the triangular flow v_3 by using different methods for different configuration of ^{12}C structure.

dence in different p_T ranges. The elliptic flow in chain case presents slightly increasing trend with the increasing of N_{track} in lower p_T range ($0 < p_T < 1$ GeV/c) and the increasing trend becomes obvious in higher p_T range ($1 < p_T < 3$ GeV/c). And v_2 is higher by EP-method than by other methods in lower p_T range ($0 < p_T < 1$ GeV/c). In Woods-Saxon distribution and triangle pattern, in higher p_T range ($1 < p_T < 3$ GeV/c) $v_2\{EP\}$ is approximately equal to $v_2\{2\}$ and $v_2\{2, |\Delta\eta| > 2\}$ to $v_2\{PP\}$. However, in chain pattern, $v_2\{2, |\Delta\eta| > 2\}$ is lower than elliptic flow by using other methods in higher p_T range. Figure 7 shows the triangular flow as a function of N_{track} in different p_T range by the above flow analysis methods. The triangular flow presents flat N_{track} dependent trend in lower p_T range ($0 < p_T < 1$ GeV/c) and also in higher p_T range ($1 < p_T < 3$ GeV/c) for chain structure. The triangular flow increases with the increasing of N_{track} in higher p_T range ($1 < p_T < 3$ GeV/c) for Woods-Saxon distribution and triangle structure. The elliptic and triangular flow increase with N_{track} in higher p_T range ($1 < p_T < 3$ GeV/c) for some cases in 6 and figure 7. This phenomenon is related to the transformation from the coordinate anisotropy to momentum anisotropy. The participant eccentricity coefficients is defined as $\epsilon_n\{PP\} \equiv \frac{\sqrt{\langle r^2 \cos(n\phi_{part}) \rangle^2 + \langle r^2 \sin(n\phi_{part}) \rangle^2}}{\langle r^2 \rangle}$. The $\epsilon_2\{PP\}$ and $\epsilon_3\{PP\}$ were calculated in the impact parameter b range (0,4) fm corresponding to N_{track} range (220,440) and there was no obvious b (N_{track}) dependence of $\epsilon_2\{PP\}$ and $\epsilon_3\{PP\}$. Table I shows the value of $\epsilon_2\{PP\}$ and $\epsilon_3\{PP\}$ for difference config-

TABLE I: Participant eccentricity coefficients for different configuration cases.

	$\epsilon_2\{PP\}$	$\epsilon_3\{PP\}$
Chain	0.5	0.16
Triangle	0.23	0.25
Woods-Saxon	0.26	0.22

uration cases. This implies that transformation from the coordinate anisotropy to momentum anisotropy depends on the number of particles created in the system, such as N_{track} , which is consistent with that from reference [12, 17, 58, 59]. From different method comparing, it can be found that $v_3\{2, |\Delta\eta| > 2\}$ takes the lowest value in triangle pattern in higher p_T range for the non-flow contribution is omitted effectively.

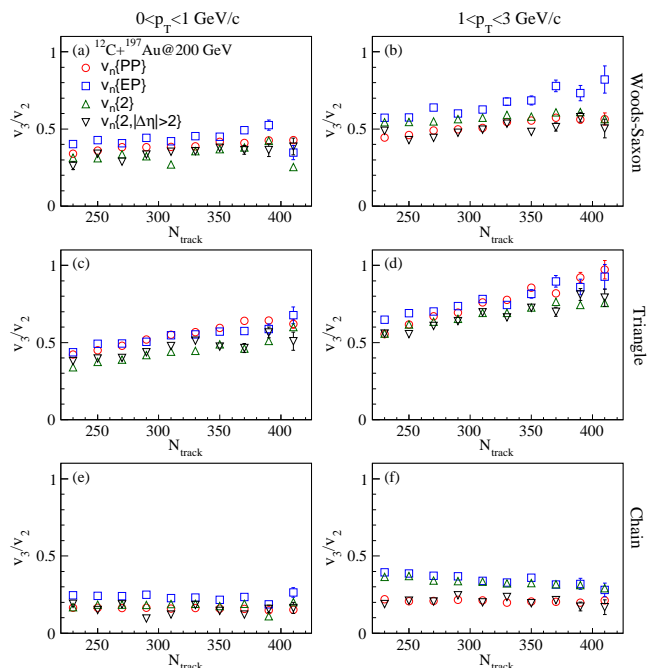


FIG. 8: (color online) In $^{12}\text{C}+^{197}\text{Au}$ collisions at $\sqrt{s_{NN}} = 200$ GeV, the ratio of v_3/v_2 by using different methods for different α -clustering configuration of ^{12}C structure.

As we mentioned in our previous work [23], v_3/v_2 can be a probe to distinguish the geometry pattern of ^{12}C through collective flow measurements. In this work we calculated the probe by using different flow calculation/measurement method as shown in figure 8. In Woods-Saxon distribution pattern, the ratio of v_3/v_2 keeps flat with the increasing of N_{track} by using PP-method, QC-method and 2PC-method, but by using EP-method v_3/v_2 increases with the increasing of N_{track} . In triangle pattern, v_3/v_2 presents increasing trend with the increasing of N_{track} by using different flow calculation method. And in chain pattern, the ratios of v_3/v_2 through PP-method and 2PC-method keep flat with the

increasing of N_{track} , but the ratios through EP-method and QC-method slightly decrease with the increasing of N_{track} . So we can conclude that the ratio of v_3/v_2 from the 2PC-method is closest to that from the PP-method and we propose to investigate the α -clustering nuclear structure by flow measurement in heavy-ion collisions. To distinguish α -clustering nuclear structure by v_3/v_2 in experiment, non-exotic structure nucleus near ^{12}C colliding against ^{197}Au can be a reference collision system. If v_3/v_2 in $^{12}\text{C}+^{197}\text{Au}$ collisions is close to that in the reference system, ^{12}C will be in non-exotic nuclear structure. If v_3/v_2 in $^{12}\text{C}+^{197}\text{Au}$ collisions is obviously smaller than that in the reference system, ^{12}C should be in three α -clusters chain structure. And if v_3/v_2 in $^{12}\text{C}+^{197}\text{Au}$ collisions is significantly increasing with N_{track} , ^{12}C can be seen as a triangle shape with three α -clusters.

IV. SUMMARY

In summary, participant plane, event plane, Q-cumulant and two particle correlation with $\Delta\eta$ gap methods were employed to calculate the elliptic and triangular

flow coefficients in $^{12}\text{C}+^{197}\text{Au}$ collisions at $\sqrt{s_{NN}} = 200$ GeV with α -clustering ^{12}C structure arranged in triangle, chain and Woods-Saxon distributions, respectively. The ratio of v_3/v_2 was proposed as a probe to distinguish the pattern of α -clustered ^{12}C structure. By using two-particle correlation method with $\Delta\eta$ gap the ratio is closest to that by using participant plane method. And v_3/v_2 can be measured in relativistic nucleus-nucleus collisions by two-particle correlation method with $\Delta\eta$ gap and as well as 4- or more-particle cumulant method is alternative if it works well for this small system.

We are grateful for discussion with Dr. Aihong Tang from BNL. This work was supported in part by the National Natural Science Foundation of China under contract Nos. 11421505, 11220101005, 11775288 and U1232206, the Major State Basic Research Development Program in China under Contract No. 2014CB845400, and the Key Research Program of Frontier Sciences of the CAS under Grant No. QYZDJ-SSW-SLH002, and National Key R&D Program of China under Grant No. 2016YFE0100900.

-
- [1] L. Adamczyk et al. (STAR Collaboration), Phys. Rev. Lett. **112**, 162301 (2014).
 - [2] L. Adamczyk et al. (STAR Collaboration), Phys. Rev. C **88**, 014902 (2013).
 - [3] L. Adamczyk et al. (STAR Collaboration), Phys. Rev. C **88**, 014904 (2013).
 - [4] L. Adamczyk et al. (STAR Collaboration), Phys. Rev. Lett. **114**, 252302 (2015).
 - [5] L. Adamczyk et al. (STAR Collaboration), Phys. Rev. C **92**, 014904 (2015).
 - [6] A. Adare et al. (PHENIX Collaboration), arXiv:1410.2559 (2014).
 - [7] L. Adamczyk et al. (STAR Collaboration), Phys. Rev. C **92**, 021901(R) (2015).
 - [8] R. D. de Souza, J. Takahashi, T. Kodama, and P. Sorensen, Phys. Rev. C **85**, 054909 (2012).
 - [9] A. Chaudhuri, Phys. Lett. B **710**, 339 (2012).
 - [10] H. Song, S. A. Bass, and U. Heinz, Phys. Rev. C **83**, 054912 (2011).
 - [11] S. Floerchinger and U. A. Wiedemann, Phys. Lett. B **728**, 407 (2014).
 - [12] P. Bożek, W. Broniowski, E. R. Arriola, et al., Phys. Rev. C **90**, 064902 (2014).
 - [13] W. Broniowski and E. R. Arriola, Phys. Rev. Lett. **112**, 112501 (2014).
 - [14] L. Ma, G. L. Ma, and Y. G. Ma, Phys. Rev. C **94**, 044915 (2016).
 - [15] L. Ma, G. L. Ma, and Y. G. Ma, Phys. Rev. C **89**, 044907 (2014).
 - [16] L. X. Han, G. L. Ma, Y. G. Ma, et al., Phys. Rev. C **84**, 064907 (2011).
 - [17] H.-C. Song, Y. Zhou, and K. Gajdosova, Nucl. Sci. Tech. **28**, 99 (2017).
 - [18] J. Wang, Y. G. Ma, G. Q. Zhang, et al., Nucl. Sci. Tech. **24**, 030501 (2013).
 - [19] C. C. Guo, W. B. He, and Y. G. Ma, Chin. Phys. Lett. **34**, 092101 (2017).
 - [20] X.-F. Luo and N. Xu, Nucl. Sci. Tech. **28**, 112 (2017).
 - [21] C. M. Ko and F. Li, Nucl. Sci. Tech. **27**, 140 (2016).
 - [22] Q. Y. Shou, G. L. Ma, and Y. G. Ma, Phys. Rev. C **90**, 047901 (2014).
 - [23] S. Zhang, Y. G. Ma, J. H. Chen, W. B. He, and C. Zhong, Phys. Rev. C **95**, 064904 (2017).
 - [24] F. D. Murnaghan, Bull. Amer. Math. Soc. **39**, 487 (1933).
 - [25] W. B. He, Y. G. Ma, X. G. Cao, X. Z. Cai, and G. Q. Zhang, Phys. Rev. Lett. **113**, 032506 (2014).
 - [26] W. B. He, Y. G. Ma, X. G. Cao, et al., Phys. Rev. C **94**, 014301 (2016).
 - [27] B. S. Huang, Y. G. Ma, and W. B. He, Phys. Rev. C **95**, 034606 (2017).
 - [28] B. S. Huang, Y. G. Ma, and W. B. He, Eur. Phys. J. A **53**, 119 (2017).
 - [29] S. A. Voloshin, A. M. Poskanzer, A. Tang, et al., Phys. Lett. B **659**, 537 (2008).
 - [30] B. Alver and G. Roland, Phys. Rev. C **81**, 054905 (2010).
 - [31] R. A. Lacey, R. Wei, J. Jia, et al., Phys. Rev. C **83**, 044902 (2011).
 - [32] J.-Y. Ollitrault, Phys. Rev. D **46**, 229 (1992).
 - [33] A. M. Poskanzer and S. A. Voloshin, Phys. Rev. C **58**, 1671 (1998).
 - [34] S. Afanasiev et al. (PHENIX Collaboration), Phys. Rev. C **80**, 024909 (2009).
 - [35] L. Adamczyk et al. (STAR Collaboration), Phys. Rev. C **86**, 054908 (2012).
 - [36] L. Adamczyk et al. (STAR Collaboration), Phys. Rev. C **88**, 014904 (2013).
 - [37] A. Bilandzic, R. Snellings, and S. Voloshin, Phys. Rev. C **83**, 044913 (2011).

- [38] G. Aad et al. (ATLAS Collaboration), Phys. Rev. C **86**, 014907 (2012).
- [39] S. Chatrchyan et al. (CMS Collaboration), Eur. Phys. J C **72**, 1 (2012).
- [40] S. Chatrchyan et al. (CMS Collaboration), Phys. Lett. B **724**, 213 (2013).
- [41] A. Bzdak and G.-L. Ma, Phys. Rev. Lett. **113**, 252301 (2014).
- [42] V. Khachatryan et al. (CMS Collaboration), Phys. Lett. B **765**, 193 (2017).
- [43] Z.-W. Lin, C. M. Ko, B.-A. Li, et al., Phys. Rev. C **72**, 064901 (2005).
- [44] G.-L. Ma and Z.-W. Lin, Phys. Rev. C **93**, 054911 (2016).
- [45] Z.-w. Lin, C. M. Ko, and S. Pal, Phys. Rev. Lett. **89**, 152301 (2002).
- [46] G.-L. Ma, S. Zhang, Y.-G. Ma, et al., Phys. Lett. B **641**, 362 (2006).
- [47] B. I. Abelev and *et al.* (STAR Collaboration) (STAR Collaboration), Phys. Rev. Lett. **101**, 252301 (2008).
- [48] A. Bzdak and G.-L. Ma, Phys. Rev. Lett. **113**, 252301 (2014).
- [49] X.-H. Jin, J.-H. Chen, Y.-G. Ma, et al., Nucl. Sci. Tech. **29**, 54 (2018).
- [50] X.-H. Jin, J.-H. Chen, Z.-W. Lin, et al., Sci. China (2018).
- [51] X.-N. Wang and M. Gyulassy, Phys. Rev. D **44**, 3501 (1991).
- [52] M. Gyulassy and X.-N. Wang, Computer Physics Communications **83**, 307 (1994).
- [53] B. Zhang, Computer Physics Communications **109**, 193 (1998).
- [54] B.-A. Li and C. M. Ko, Phys. Rev. C **52**, 2037 (1995).
- [55] T. Maruyama, K. Niita, and A. Iwamoto, Phys. Rev. C **53**, 297 (1996).
- [56] L. He, T. Edmonds, Z.-W. Lin, F. Liu, D. Molnar, and F. Wang, Phys. Lett. B **753**, 506 (2016).
- [57] G.-L. Ma and A. Bzdak, Nucl. Phys. A **956**, 745 (2016).
- [58] F. G. Gardim, F. Grassi, M. Luzum, and J.-Y. Ollitrault, Phys. Rev. C **85**, 024908 (2012).
- [59] H. Niemi, G. S. Denicol, H. Holopainen, and P. Huovinen, Phys. Rev. C **87**, 054901 (2013).